



## Highly Efficient Flyback Microinverter for Photovoltaic Applications

<sup>1</sup>Vandana Kushwaha, <sup>2</sup>Prof. Indrajeet Kumar, <sup>3</sup>Prof. Priyank Gour

<sup>1</sup>M.Tech Scholar, <sup>2</sup>Assistant Professor, <sup>3</sup>Assistant Professor & HOD

Department of Electrical & Electronics Engineering

SCOPE College of Engineering, Bhopal, India

**Abstract :** A highly efficient flyback microinverter is a specialized device, which is used to convert direct current (DC) power generated by solar panels into alternating current (AC) power suitable for grid-connected applications. The microinverter technology has gained popularity in recent years due to its advantages over traditional central inverters, especially when it comes to system performance, flexibility, and reliability. This paper presents the highly efficient flyback microinverter for photovoltaic applications. Design and simulation of the present model is performed using MATLAB software.

**Index Terms –** Flyback, Ratio, Micro-inverter, Voltage, Gain.

### I. INTRODUCTION

A solar micro-inverter, or simply microinverter, is a plug-and-play device used in photovoltaics, that converts direct current (DC) generated by a single solar module to alternating current (AC). Microinverters contrast with conventional string and central solar inverters, in which a single inverter is connected to multiple solar panels. The output from several microinverters can be combined and often fed to the electrical grid. For photovoltaic applications, the flyback micro-inverter with pseudo DC link is popular as a simple topology but brings large transformer turns ratio and thus large leakage inductance, which would deteriorate the converter efficiency. To solve this issue, based on the non-isolated pseudo-dc-link structure, this research present a highly efficient boost-flyback/flyback (BF/F) micro-inverter. This new topology is operated at BF mode for the most segment of a half grid cycle and F mode for the rest. During the BF mode, high voltage gain with low voltage stress is easily available in minimized transformer turns ratio. Besides, the leakage energy is recycled and the turn-off voltage spike of main switch is clamped, as a result of a passive snubber inherently contained in this mode.

In recent years, renewable energy sources have gained significant traction as the world's collective efforts to combat climate change have intensified. Among these sources, solar energy stands out as one of the most promising and readily available options. Solar photovoltaic (PV) systems, which convert sunlight into electricity, have become increasingly popular for residential, commercial, and industrial applications. A key component that has played a crucial role in the advancement of solar energy systems is the flyback microinverter.

Traditionally, solar PV systems used central or string inverters to convert the DC output from multiple solar panels into AC power for grid integration. However, advancements in power electronics have led to the development of microinverters that offer several advantages over their central counterparts. A flyback microinverter, in particular, stands out for its efficiency, reliability, and ability to improve overall system performance.

The flyback microinverter is based on the flyback topology, a type of switching power supply circuit. It employs a transformer to provide electrical isolation between the input (solar panels) and output (grid or loads). The basic working principle involves a series of steps:

1. **DC-to-DC Conversion:** The DC voltage generated by a single solar panel or a small group of panels is connected to the input side of the microinverter.
2. **High-Frequency Switching:** The microinverter uses high-frequency switching devices, typically MOSFETs or IGBTs, to control the flow of current through the transformer primary winding.
3. **Energy Storage:** During the switch's ON state, energy is stored in the transformer's magnetic field. When the switch turns OFF, the energy is transferred to the secondary winding.
4. **Voltage Transformation:** The transformer provides voltage transformation to step up or step down the input DC voltage to the required output AC voltage.
5. **AC Output:** The transformed AC voltage is filtered and conditioned to produce a clean sinusoidal output, which is then connected to the electrical grid or local loads.

## II. PRESENT WORK

The present work can be understood by using following flow chart-

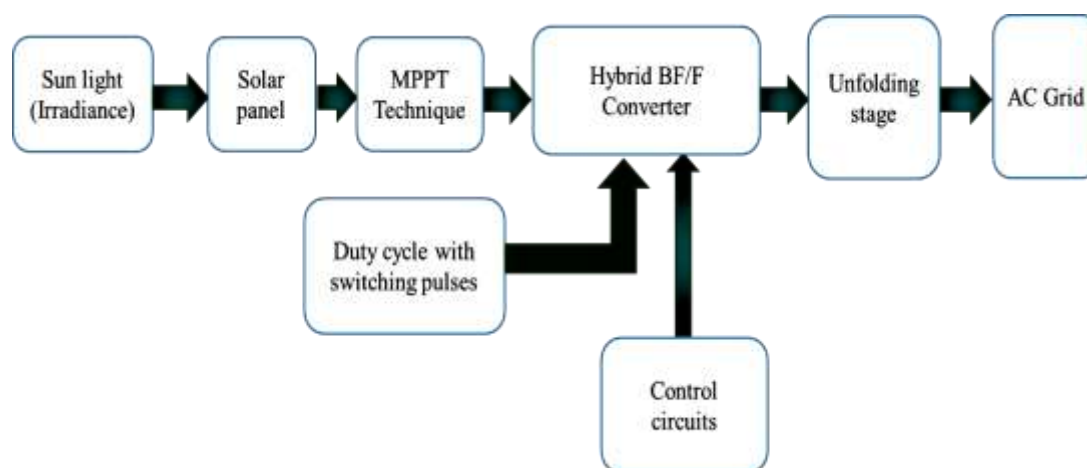


Figure 1: Flow Chart

The present efficient BF/F miniature inverter with non-detached pseudo DC interface, which comprises of an exceptionally BF/F converter and an unfolding stage. The hybrid BF/F converter is involved a decoupling capacitor  $C_i$ , a primary power switch  $Q_1$ , a resonating capacitor  $C_s$ , two power rectifier diodes  $D_1$  and  $D_2$ , two yield filter capacitors  $C_1$  and  $C_2$ , a coupled transformer  $T$  that is modeled as a polarizing inductor  $L_m$ , a leakage inductor  $L_s$ , and an ideal transformer with the turns proportion  $N$ , and an activity mode progress network that is made out of two switches  $Q_2$  and  $Q_3$  reciprocally worked at twofold line frequency. The unfolding stage incorporates four switches  $S_1$ ,  $S_2$ ,  $S_3$  and  $S_4$  worked at line frequency, a filter capacitor  $C_f$  and a filter inductor  $L_f$ . If the switch  $Q_2$  is ON and  $Q_3$  is OFF, at that point the miniature inverter is in BF mode, in any case, the miniature inverter is in F mode.

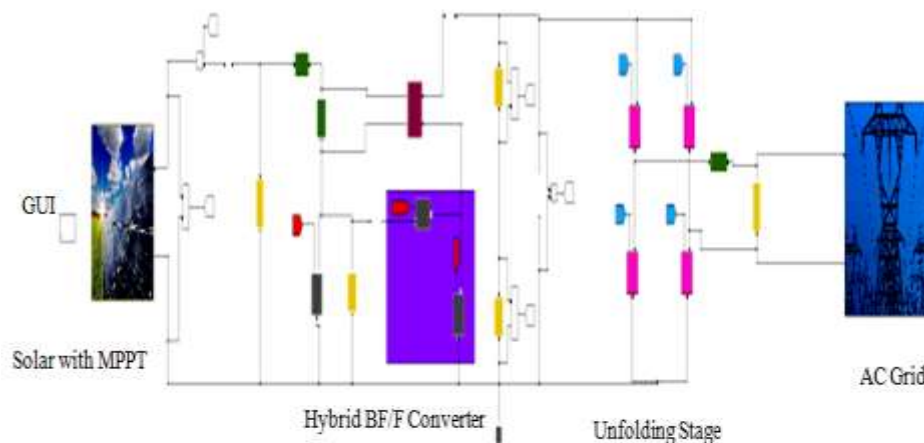


Figure 2: Present Model

Figure 2 is showing the present models details. The BCM activity with top current control is received, since it offers high power thickness and transformation efficiency, and it likewise gives regular soft-exchanging of power gadgets, including ZVS and Versus of the primary switch  $Q_1$ , and ZCS of the rectifier diodes  $D_1$  and  $D_2$ , with the QR method utilized. The miniature inverter works at BF mode when  $v_o > V_i + \Delta V$ , where  $v_o$  is the yield voltage of the circuit,  $V_i$  is the normal worth of the information voltage  $v_i$ , and  $\Delta V$  is a steady voltage esteem. During this mode, the switch  $Q_2$  is consistently ON and the  $Q_3$  is OFF, which makes the sub-boost converter effectively share the high prompt power with the sub-flyback converter. The boost inductor and the flyback transformer are coupled into the transformer  $T$ , and the yield voltage  $v_o$  is acquired by falling the yield voltages ( $v_{c1}$ ,  $v_{c2}$ ) of the two sub-converters. Therefore, high voltage acquire is achieved with low voltage weight on the principle switch  $Q_1$ , the two rectifier diodes  $D_1$  and  $D_2$ , and the two yield capacitors  $C_1$  and  $C_2$ . Then again, this mode intrinsically gives a latent snubber, which is made out of the diode  $D_2$ , and the capacitors  $C_s$  and  $C_2$ . Henceforth, the energy put away in the leakage inductor  $L_s$  is reused to the yield side. Then, the voltage overshoot of the fundamental switch  $Q_1$  is stifled during the mood killer measure. Since the yield voltage  $v_o$  can't be controlled lower than the information voltage  $v_i$  during the BF mode, the F mode is created with the switch  $Q_3$  consistently ON and the  $Q_2$  OFF.

This mode is around the zero grid voltage, where the prompt transferred power is low. Therefore, the effect of the leakage inductor can be disregarded. Notwithstanding, because of the fact that the exchanging frequency during this mode is very higher than the BF mode, its term, which is controlled by  $\Delta V$ , should be fittingly confined to the most limited conceivable time. The full capacitor  $C_s$  is included corresponding with the fundamental switch  $Q_1$  for offering an appropriate QR time. It helps the time deferral of turn-on driving signal be planned flexibly, so the ZVS or Versus turn-on in BCM activity is ensured. In addition, this capacitor effectively improves the mood killer measure by bringing down the rising incline of the voltage across  $Q_1$ .

III. SIMULATION RESULTS

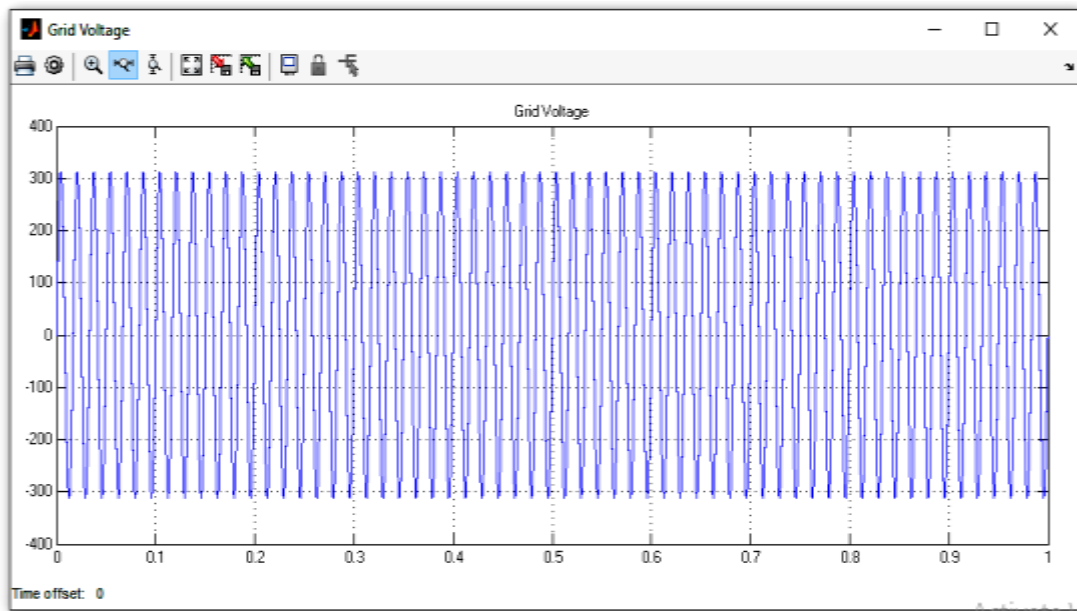


Figure 3: Grid Voltage

Figure 3 is showing the value of grid voltage. It is generated from the overall microinverter system. The value of grid voltage is 320V.

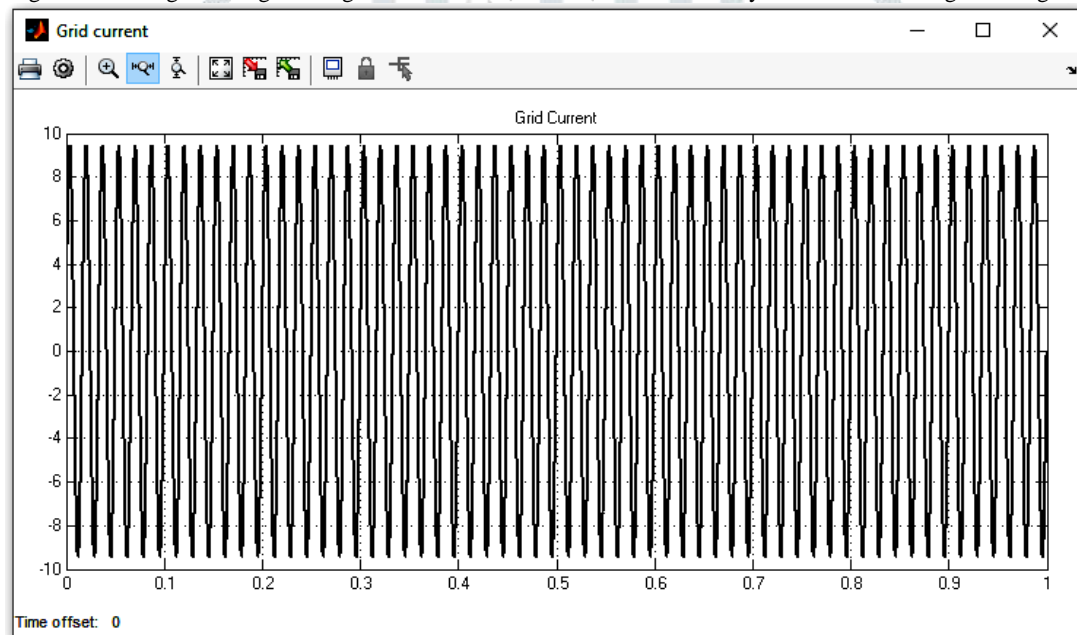


Figure 4: Grid Current

Figure 4 is showing the value of grid current. It is generated from the overall microinverter system. The value of grid current is 9.5A.

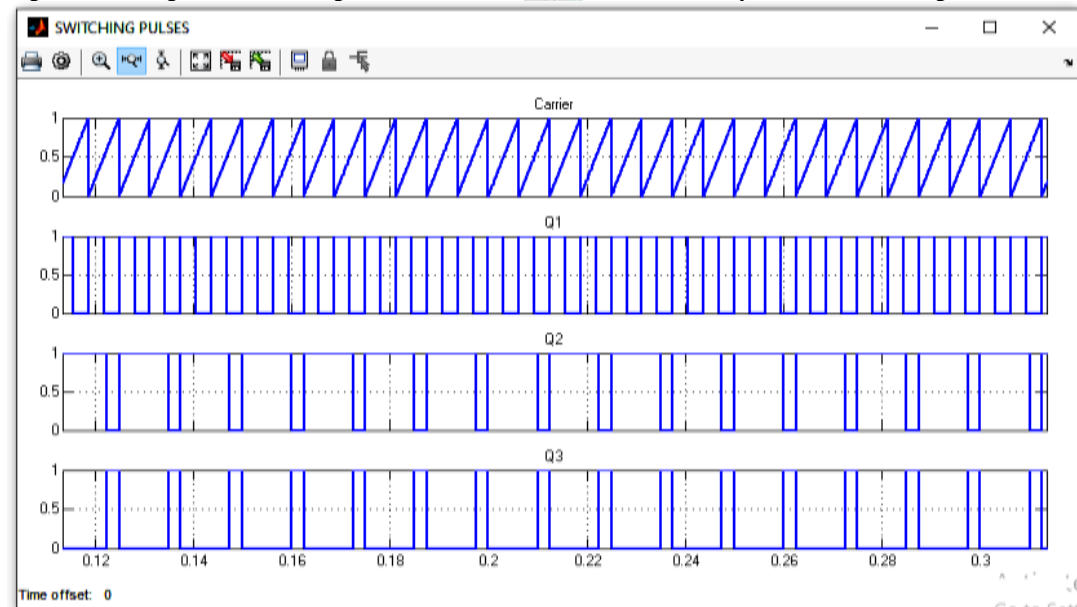


Figure 5: Switching pulse

Figure 5 is showing the switching pulse. The Q1, Q2 and Q3 are the various switches signals and carrier wave. It is used to switching pulse of the signal.

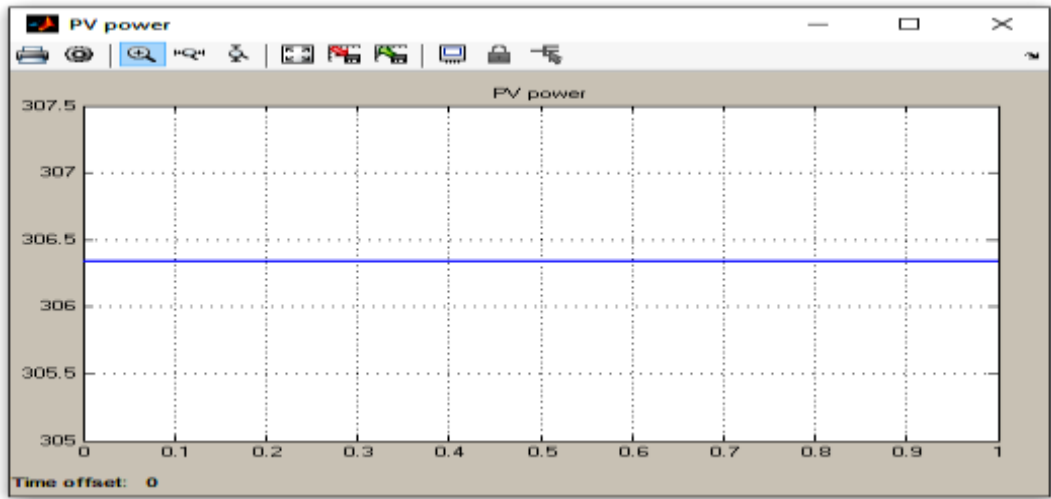


Figure 6: PV Power

Figure 6 is showing the PV power of the present model. The value of the PV power is the 306.4 W.

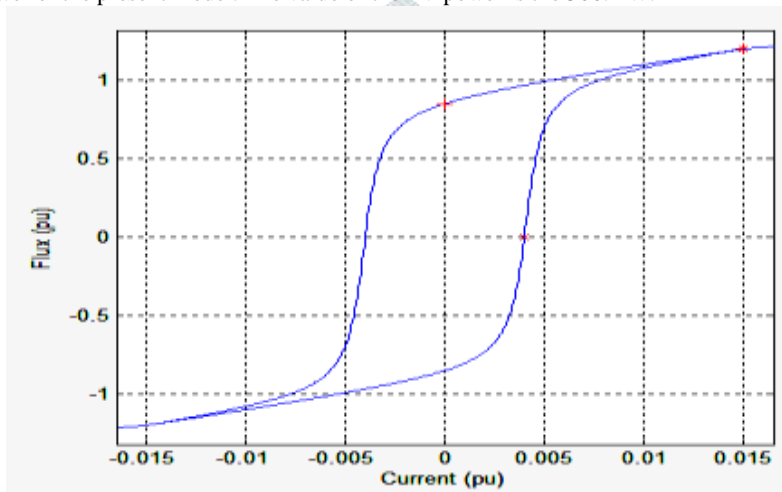


Figure 7: Hysteresis curve

Figure 7 is showing the hysteresis curve regarding the current and flux esteems. A hysteresis circle shows the connection between the incited magnetic flux thickness B and the polarizing force H.

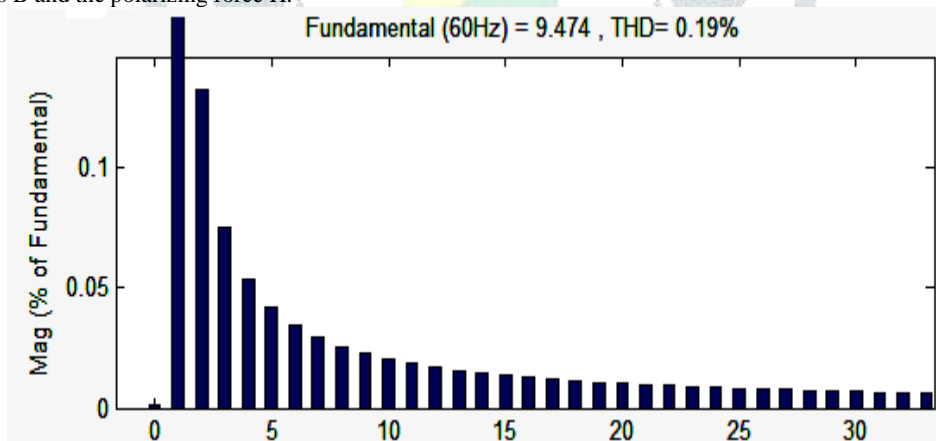


Figure 8: Total Harmonic Distortion

Figure 8 is showing the all out consonant bending of the current model as far as the sounds request. The worth of THD is the 0.19%. The current work offers the base benefit of the THD. It is an estimation of the symphonious contortion present in a signal and is defined as the proportion of the amount of the powers of all consonant parts to the power of the fundamental frequency.

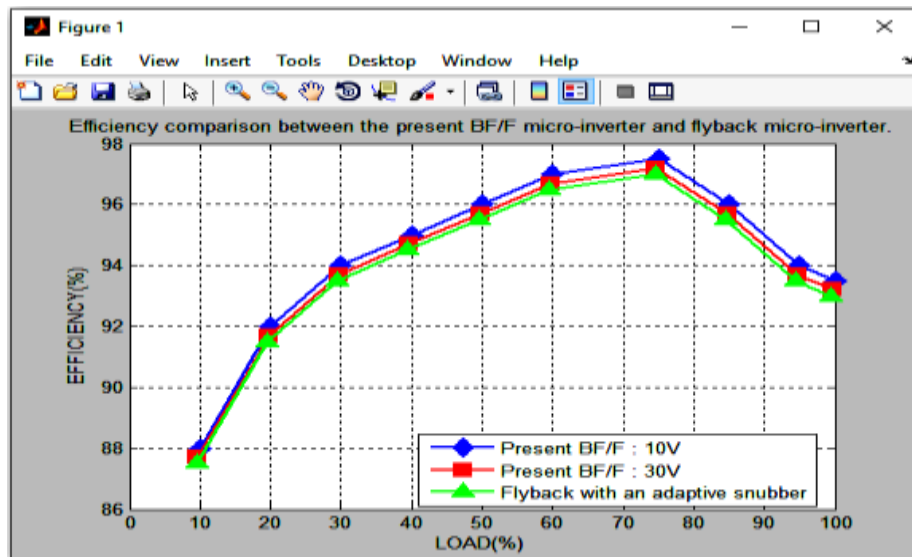


Figure 9: Efficiency comparison between the present BF/F micro-inverter and flyback micro-inverter

Figure 9 is introducing the examination of efficiency of present and past approach. The efficiencies at all heaps of the present BF/F miniature inverter are higher than those of the flyback miniature inverter. In addition, they are further improved when  $\Delta V$  is decreased from 30V to 10V. The maximum efficiency of the present miniature inverter is 97.5% ( $\Delta V=10V$ ), while the one of the flyback miniature inverter is simply 97%.

Table 1: Results comparison

Sr. No	Parameter	Previous Model	Present Model
1	Grid Voltage	220V	320V
2	Output Power	240W	306.4 W
3	THD	2.175 %	0.19%
4	Efficiency	96.2%	97.5%

Table 1 is showing the results comparison of the previous and present model. The present model grid voltage is the 320V while previously it is 220V.

**IV. CONCLUSION**

Flyback microinverters have emerged as a game-changing technology in the field of solar energy conversion. Their ability to maximize power output, improve system efficiency, and enhance safety has made them increasingly popular in solar PV installations. As the world seeks sustainable and eco-friendly energy solutions, flyback microinverters, along with other advancements in solar technology, are likely to play a crucial role in shaping the future of renewable energy. The present model grid voltage is the 320V while previously it is 220V. The output power is the 306.4W while previously it is 240W. The total harmonic distortion is the 0.19% while previously it is 2.175 %. The overall efficiency is the 97.5% while previously it is 96.2%. Therefore the simulation results show that the present model is achieving the significant better results than existing approaches.

**REFERENCES**

1. F. Zhang, Y. Xie, Y. Hu, G. Chen and X. Wang, "A Hybrid Boost-Flyback/Flyback Microinverter for Photovoltaic Applications," in IEEE Transactions on Industrial Electronics, vol. 67, no. 1, pp. 308-318, Jan. 2020, doi: 10.1109/TIE.2019.2897543.
2. F. Ronilaya, S. B. Kurniawan, M. N. Hidayat, E. Rohadi, R. Sutjipto and I. Siradjuddin, "A Power Sharing Loop Control Method for Input-series Output-parallel Flyback-type Micro-Inverter Using Droop Method," 2019 International Conference on Information and Communications Technology (ICOIACT), Yogyakarta, Indonesia, 2019, pp. 823-828, doi: 10.1109/ICOIACT46704.2019.8938411.
3. C. Chen, J. Li, S. Gao and Y. Ma, "Design of Staggered Fly-back Single-phase Photovoltaic Grid-connected Micro-inverters," 2019 IEEE 3rd Information Technology, Networking, Electronic and Automation Control Conference (ITNEC), Chengdu, China, 2019, pp. 1793-1798, doi: 10.1109/ITNEC.2019.8729402.
4. F. Zhang, Y. Xie, Y. Hu, G. Chen and X. Wang, "A Novel Dual-mode Micro-inverter for Photovoltaic AC Module Applications," 2019 IEEE Applied Power Electronics Conference and Exposition (APEC), Anaheim, CA, USA, 2019, pp. 127-132, doi: 10.1109/APEC.2019.8722184.
5. N. Singh and P. G. P. Pandiya, "Interpretation of MPPT Techniques in Grid Connected Solar PV Array System", IJOSTHE, vol. 5, no. 6, p. 5, Feb. 2019. <https://doi.org/10.24113/ojssports.v5i6.96>
6. E. KABALCI and A. BOYAR, "Design and Analysis of a Single Phase Flyback Micro Inverter," 2018 6th International Conference on Control Engineering & Information Technology (CEIT), Istanbul, Turkey, 2018, pp. 1-6, doi: 10.1109/CEIT.2018.8751843.
7. R. de Oliveira Lima, L. H. S. C. Barreto and F. E. U. Reis, "Hybrid MPPT Control Applied to a Flyback Micro-Inverter Connected the Electrical Grid," 2018 13th IEEE International Conference on Industry Applications (INDUSCON), São Paulo, Brazil, 2018, pp. 59-64, doi: 10.1109/INDUSCON.2018.8627283.
8. N. Falconar, D. S. Beyragh and M. Pahlevani, "A novel control system for solar tile micro-inverters," 2018 IEEE Applied Power Electronics Conference and Exposition (APEC), San Antonio, TX, 2018, pp. 375-380, doi: 10.1109/APEC.2018.8341038.
9. D. Voglitsis, N. Papanikolaou and A. C. Kyritsis, "Incorporation of Harmonic Injection in an Interleaved Flyback Inverter for the Implementation of an Active Anti-Islanding Technique," in IEEE Transactions on Power Electronics, vol. 32, no. 11, pp. 8526-8543, Nov. 2017, doi: 10.1109/TPEL.2016.2646419.
10. H. A. Sher, A. A. Rizvi, K. E. Addoweesh and K. Al-Haddad, "A Single-Stage Stand-Alone Photovoltaic Energy System With High Tracking Efficiency," in IEEE Transactions on Sustainable Energy, vol. 8, no. 2, pp. 755-762, April 2017, doi: 10.1109/TSTE.2016.2616443.
11. F. Karbakhsh, M. Amiri and H. Abootorabi Zarchi, "Two-switch flyback inverter employing a current sensorless MPPT and scalar control for low cost solar powered pumps," in IET Renewable Power Generation, vol. 11, no. 5, pp. 669-677, 12 4 2017, doi: 10.1049/iet-rpg.2016.0631.